Small Molecule Activators of PP2A Suggests Controlled Tau Phosphorylation as a Novel Mode of therapy for Alzheimer's disease

Jagadeesh Kumar.D,* Mohammed Toufiq, Priya Narayan & H G Nagendra

Department of Biotechnology, Sir M. Visvesvaraya Institute of Technology,

Bangalore-562 157, India

*Corresponding Author

 Jagadeesh kumar.D

Email: jk4you@gmail.com

ABSTRACT

Alzheimer's disease (AD) is characterized by neurofibrillary tangles (NFTs), formed as a consequence of hyperphosphorylation of tau. The extent of phosphorylation of tau is regulated by protein phosphatases (PPs) like PP1, PP2A/Bα, PP2B and PP5. Interestingly, PP2A/Bα, is a major brain tau phosphatase which account for 70% of the dephosphorylation events in brain and, its activity is known to decrease by half under AD conditions. The down regulation of PP2A leads to hyperphosphorylation of Tau in the brains of AD patients. Hence, the process of reversal of tau phosphorylation needs to be achieved by the activation of PP2A, through specific molecules, as this could pave way towards development of novel therapeutics for AD. The key objective of the current study was thus to understand the affinities of various small molecules that could function as potential activators of PP2A. Molecules like Xylulose-5-Phosphate, Dihydroxy Phenylethanol, EGCG, Memantine, Sodium Selenate, Tetralone and Quinolone exhibit strong interactions across identified binding pockets of PP2A. The investigation not only confers that there could be more than one activation site in PP2A, but also offers clues as to how

these molecules facilitate restoration of the phosphatases activity, thus proposing newer avenues for the treatment of AD.

KEYWORDS: Alzheimer's disease, Tau, Dephosphorylation, Hyperphosphorylation, PP2A, Small Molecule Activators, Memantine.

Running Title: Small Molecule Activators of PP2A in Alzheimer's disease

1. INTRODUCTION

Alzheimer's disease (AD) is the most common form of neurodegenerative disorder (NDD) characterized by the incidence of two major diagnostic hallmarks composed of β-amyloid (Aβ) deposits and intracellular Neurofibrillary tangles (NFTs) [1]. In normal neurons, a microtubule-associated phosphoprotein Tau (MAPT) is found mostly in the axons of central nervous system, where it controls the length / stability and also assists in transport of material to and from the cell body to the synapse [2]. In AD pathogenesis, this MAPT (tau) gets abnormally hyperphosphorylated by the action of several different tau kinases resulting in their misfolding, aggregation and formation of NFTs[3]. The NFTs comprises of bundles of paired helical filaments (PHFs) and straight filaments that cause neurodegeneration in the hippocampus, resulting in memory deficit and eventual neuronal cell death. In spite of in-depth knowledge, drug discovery approaches involving the amyloid cascade hypothesis has not been efficacious[4]. Hence, alternative approaches for tackling AD needs to be attempted with tau hypothesis.

In the brain, tau is vulnerable to a large number of different kinases and phosphatases that control phosphorylation and dephosphorylation events. During AD pathogenesis, due to altered expressions of major tau kinases like GSK3β, CDK5, Dyrk1A, JNKp38, AKT1 etc., uncontrolled phosphorylation occurs in tau at the 85 odd potential sites involving serines (S), threonines (T), and tyrosines (Y) residues[4]. Because of this dysregulation of kinases and

decreased activity of phosphatases, that causes hyperphosphorylation of tau, cascade of events like tau dissociation, insoluble tau aggregation, microtubules disintegration, and neuronal death occur sequentially[5]. It is also known that, about 2–3 moles of phosphate per mole of tau can be detected under normal conditions, while during pathological environments; this proportion is amplified to 7–8 times[6, 7, 8].

The events of phosphorylation and dephosphorylation of proteins are the important mechanisms for cellular regulation. Phosphatases are equivalent of kinases, and remain responsible for the dephosphorylation of many different intracellular molecules including tau, under normal conditions. Progress in the structure and mechanism of phosphatases, have indicated that these enzymes are specifically controlled, and are as essential as kinases, in the regulation of dephosphorylation events[9]. Only a few serine/threonine phosphatases (PSPs) control the specific dephosphorylation of thousands of phosphoprotein substrates[10]. However, in the brains of AD patients, expression and/or total phosphatase activity of Tau protein phosphatases (PPs) like protein phosphatase 1 (PP1), Protein phosphatase 2A (PP2A/Bα), PP5 and PTEN are decreased by half, although the activities of PP2B (calcineurin), Cdc25A, Cdc25B are up regulated[4,5]. PP2A accounts for as much as 1% of the total cellular proteins[10] (Shi, 2009), and along with PP1, they account for >90% of all Ser/Thr phosphatase activities in AD tissues and cells[11]. Among the protein phosphatases involved in Tau dephosphorylation, PP2A has been shown to be the most important and a key phosphatase, which alone accounts for over ~70% of tau dephosphorylation[12]. Though the down regulation of PP2A activity appears to cause hyperphosphorylation of Tau in the brains of AD patients, the underlying mechanism of altered phosphatase activity remains unexplored[13].

Phosphatases have been less studied, mostly due to their complex regulatory mechanisms. Current pharmacological approaches in reduction of Tau phosphorylation involves, inhibition of specific kinases via small molecules that are developed as targets for drug development[14]. However, the results have been unsatisfactory because of involvement of kinases in numerous other biological processes, and a specific binding of its inhibitors to non-disease targets leads to adverse effects and, due to active site similarity and inhibitor specificity. Hence, as an alternative strategy to kinase inhibition, we propose to screen pharmacological compounds that could enable increase or at least restore the activity of tau phosphatases (specifically the major phosphatase PP2A) and revive the dephosphorylation events of tau. In addition, PP2A activation might offer possible promising effects, in rejuvenating variety of faulty signal pathways that underlie neurodegeneration. Recent studies further highlight that, direct interaction at allosteric sites, interference of inhibitory protein–protein interactions, and alteration of post-translational modifications, are potential entry points for pharmacological enchantments of PP2A function[15]. Thus, approaches to modulate PP2A's activity may provide unique opportunities for designing pharmacological interventions to tackle AD.

Realizing the need to identify the specific activators for these phosphatases, and with the expectation that it could positively affect the hyperphosphorylation of tau, the present *in silico* investigations have been undertaken. In this direction, comprehensive sequence and structural analysis of PP2A, its shared conservations across other phosphatases, studying phosphate binding site geometries, exploring alternative/allosteric binding pockets across PP2A, docking analysis with various classes of activators etc., have been methodically attempted. We have selectively screened known PP2A activators belonging to different classes like sphingoids,

phenolics, cations, anions and PP2A enhancers[16], that cross the blood–brain barrier and be able to reach the target.

Our study suggests that these set of activators share common structural features, such as distinctly lipophilic ridges or side chains with H-bond donors. An interesting set of determinants and binding residues for the various ligands have been derived. These also exhibited a range of interaction affinities across different pockets of PP2A. Key molecular interactions that could hopefully restore and/or increase the activity of phosphatases in the brain, and consequently increase the dephosphorylating activity of PP2A, have also been appreciated. Molecules like Xylulose-5-phosphate, EpiGallocatechin Gallate and Dihydroxy Phenylethano, Sodium Selenate and Memantine depict very strong interactions with PP2A, and across all binding pockets, indicating their potential exploitation as novel therapeutic agents. The analysis of these phosphatases and identification of specific small molecules as plausible activators can hopefully provide remedial solutions towards management of AD.

2. MATERIALS AND METHODS

Our research effort focuses on the *in silico* sequence and structural investigations of known four key tau Protein phosphatases comprising of PP1, PP2A, PP2B and PP5, which account for the dephosphorylation of the MAPT. Extensive sequence and structural studies were carried out by retrieving the Protein sequences from Universal Protein Resource [Uniprot][17] and their corresponding X-ray crystallography structures of the 4 human tau serine/threonine-protein phosphatases PP1 (PDB ID-3E7A), PP2A (PDB ID-3DW8), PP2B (PDB ID-1AUI), PP5 (PDB ID-1WAO) from the Protein data bank (PDB)[18]. The methodology followed in this investigation is depicted as a flow chart in **Figure 1**. The details of the molecules analyzed are provided in **Table 1**. The PP2A functions as a hetero-trimer, consisting of three subunits namely scaffold

subunit A, regulatory B-subunit and catalytic C subunit respectively. While PP1 and PP5 functions as a monomer with only the catalytic A chains, PP2B functions as a hetero-dimer with its catalytic A chain. Comparison of the catalytic C core subunit of PP2A alpha isoform with other protein human tau phosphatases, and their binding pockets, via multiple sequence alignments using MULTALIN tool[19] and its visualization with the ESPript3.0 tool[20] were carried out. The domain analysis of catalytic, Phosphate and metal binding sites of these 4 tau Proteins were also explored using the options in the tool of Discovery studio (DS) 3.5[21] and is depicted in **Figure 2**. The structural similarity of the active sites was also performed using the DS 3.5. RMSD calculations for all the catalytic subunits in these 4 protein phosphatases were calculated and are tabulated in **Table 2**. Apart from the known toxin and phosphate binding pocket, two new ligand binding sites were predicted via MetaPocket[22]. Subsequently, through extensive literature survey, various classes of activators that appear to act directly as allosteric activators of PP2A and pass through Blood Brain Barrier (BBB) were retrieved from the PubChem Compound Database[23], for docking studies. The details of these chosen inhibitors and activators are listed in **Table 5** and **Table 6** respectively. To decipher the extent of binding of these selected 8 ligands/activators with PP2A, they were docked into the identified pockets of the PP2A using FlexX[24]. These docked poses were then minimized with CHARMM force fields[25]. Candidate ligand poses were evaluated and prioritized according to the Docking Score[26]. The strength of interactions for each docked pose is tabulated in **Table 7** and **Table 8**, respectively. Similarly, for the purposes of comparison with activators, docking exercises were conducted to critically evaluate the relative binding strengths of natural toxin inhibitors as well. The molecular details of the known natural inhibitors and their docking scores are tabulated in **Table 5**. These natural toxins were selected from literatures[27] .

3. RESULTS AND DISCUSSIONS

Our efforts focus on the *in silico* sequence and structural investigations of known key tau protein phosphatases comprising of PP1, PP2A, PP2B and PP5, those account for the dephosphorylation of the MAPT. The Multiple sequence alignment of these 4 phosphatases reveals the conservation of critical amino acid residues across the catalytic subunits, phosphate binding sites and metal binding sites, respectively. The location of the conserved phosphate binding RHR amino acids (colored in RED) and metal binding residues DHNH (colored in Blue), are highlighted in **Figure 2** as rectangle boxes. The alignment reflects that the dephosphorylation and metal binding sites are well conserved across these 4 tau protein phosphatases. Likewise, the domain wise comparison amongst these phosphatases also exhibit significant commonalities as depicted in **Figure 3**. They share a common active motif consisting of G**D**X**H**G, G**D**XVD**R**G, LRG**NH**E, **H**GG, **R**G and **H**, where X refers to variable amino acids. Appreciating the sequence/domain conservations, structural homology between them was analyzed. The identity between the tau phosphatases lies between 37 to 50%, while the similarity index ranges from 67 to 77%, as indicated in **Table 2**. The RMSD between these catalytic subunit structures appear between 0.93 to 1.06 Angstroms for all C-alpha atoms, highlighting overall structural commonalities.

Since, PP2A/Bα is the main brain tau phosphatase which account for about 70% of the dephosphorylation events in brain and whose activity is known to decrease by half under AD conditions[12], we performed an in-depth investigation to appreciate the structural organization, that aid in the mechanistic understanding of its functional regulation. A systematic analysis of PP2A/Bα display that, majority of PP2A exists as a functional heterotrimer, comprising of a 36 kDa catalytic C' subunit, a 65 kDa scaffold subunit A and another regulatory B-subunit made up of 55kDa. Further, the catalytic C' subunit occurs in two isoforms namely, Cα (PPP2CA) and Cβ

(PPP2CB), and they exhibit 97% identity between them. To achieve complete activity towards substrate binding, namely tau, the PP2A C subunit associates itself with a highly diverse variable regulatory B' (Bα) subunit (PPP2R2A) to form a ABαC heterotrimeric holoenzyme[11] (refer **Figure 4**). The critical residues of Bα subunit binds and directly interacts with tau[28]. This interaction is essential for efficient dephosphorylation of tau[29]. In the nervous system, variations in this PP2A/Bα subunits expression are linked to Alzheimer's disease[30, 31]. The regulatory B-subunits are nearly 30 in number, and can be separated into four diverse gene families: B (PPP2R2/PR55), B' (PPP2R5/PR61), B" (PPP2R3/PR72/130), or B'''/striatins (PPP2R4/PR93/PR110). These regulatory B' subunit shows a little sequence similarity between families, but maintains high sequence similarity within families[32]. This subunit defines the substrate specificity and the cellular localization of PP2A by means of targeting the enzyme to different cellular compartments in the brain and by influencing the holoenzyme complex for potential substrates[33] . Similarly, the PP2A scaffold subunit occurs in two isoforms, α and β, (PPP2R1A/α and PPP2R1B/β), which are widely expressed and reveal about 86% sequence identity between them. The A-subunit is a HEAT (huntingtin-elongation-A-subunit-TOR) motif repeat containing 15 HEAT repeats arranged into an extended, L-shaped molecule and bridges interactions with catalytic and regulatory subunits responsible for the association of diverse heterotrimeric PP2A holoenzyme[34]. Further details of the subunits and their chromosome location are provided in **Table 3**.

PP2A minimally contains a well conserved catalytic subunit, the activity of which is highly regulated. Deficits in PP2A activity are linked with various factors like, down-regulation of PP2A catalytic C subunit at the gene/ protein[35] , and direct binding of specific PP2A inhibitors/ endogenous nuclear inhibitors to the catalytic subunit, rather than the PP2A regulatory

subunits PP2A-A or B. Hence, In order to investigate the potency of binding of the ligands and activators, the structural comparison of catalytic C core subunit of PP2A alpha isoform with other protein human tau phosphatases PP1, PP2B and PP5 respectively, were carried out. Molecular overlay of catalytic domain was executed using a selected set of residues surrounding the phosphate-binding site. Detailed representation of overlay is shown in **Figure 5**. The superposition highlights the conservation of 9 active site residues of PP2A, aligned with corresponding amino acids in PP1, PP2B, and PP5 respectively.

From the structural alignment, the four invariant amino acids (chosen in the order of PP2A, PP1, PP2B and PP5 respectively) viz. Arg (89, 96,122, 275), Asn (117,124,150,303), His (118,125,151,304) and Arg (214,221,254,400), substantiate the direction of the substrate for nucleophilic attack. The two metal ions manganese (II) ion ($Mn2+$) are coordinated at the active site, to mediate the phosphate transfer. The other five amino acids function as metal-coordinating residues. These nine amino acids are positioned via a compact α/β-fold composed of 11 α-helices and 14 β-strands, and is a common motif across PP2A, PP1, PP2B and PP5, respectively.

3.1 Binding Site Prediction and *In Silico* Druggability Assessment

Deciphering and understanding the functional sites is the first step to study protein function and a comprehensive knowledge of these ligand-binding sites can be vital and often a preparatory step for target-based drug design exercises, mutagenesis experiments and high-throughput virtual screening activities. With this background, identification of binding pockets and mapping of the ligand/small molecule-binding residues were carried out, to identify possible binding sites and their potential functional residues for the PP2Ac. Apart from the conventional phosphate binding pocket (pocket 1), two additional pockets (pocket 2 and pocket 3) were predicted via MetaPocket 2.0 and DS 3.5. The pocket 2 consists of 58 residues, which is found to be bigger and shallower;

and the pocket 3 contains 17 amino acid residues, and is relatively small. The details of these pockets and their pharmacophoric residues are shown in **Figure 6** and **Table 4**, respectively.

It is well-known from several literatures that, like several PPP enzymes, the PP2Ac catalytic domain is wide-open to inhibition by popular natural toxins and inhibitors such as okadaic acid, nodularin, calyculinA, microcystin-LR, and tautomycin[27]. Some of these toxins are produced by dinoflagellates and can be found in various species of shellfish, molluscs such as oysters, mussels, scallops, clams etc. It is well established in medicinal chemistry that the toxins from these species inhibit PPP family members[27] . Human consumption of contaminated bivalve molluscs such as mussels, scallops, oysters or clams contain these lipophilic and heat stable toxins, which lead to inhibition of serine/threonine protein phosphatases[27]. Molecular level appreciations of the interactions of these toxins with the residues in the pocket 1 of PP2A are still unclear.

3.2 PP2A Pocket 1– Inhibitor Interactions

Hence, in order to decipher the nature of interaction of these toxins with the residues belonging to pocket 1 of PP2A, docking exercises were undertaken. The docking results with selected toxin inhibitors, is shown in the **Table 5**. The docked molecules Fostriecin, Cantharidin, Thyrsiferyl-23-Acetate, Okadaic Acid and Microcystins-Lr appear to bind into or adjacent to the phosphate binding site, and appear to block the C subunit active site. All the inhibitors share a common binding site comprising of residues like R89, H118, H191, G193, P213, R214, G217, L243, and C269 that are part of the phosphate binding pharamacophore, as well. These results have enabled us to appreciate the molecular level interactions and the plausible inhibition of PP2A.

In view of the need to trigger the activity of PP2A towards the novel strategy of therapeutic interventions to AD, screening of activators that enhance PP2A activity with high selectivity, was adopted as the next step. Thus, our further explorations were directed towards determining the molecular basis of interactions between PP2Ac and the set of known activators, involved in enriching the function of PP2A. More than a dozen small molecules have been recognized to activate PP2A in cellular assays[15]. However, it is unclear whether they act on PP2A directly as allosteric activators, or indirectly by inhibiting the binding of PP2A inhibitors, or have any other distinct binding site etc. This question persists among scientists due to fact that the PP2A binding site is yet to be fully characterized. This demand has enabled us, to explore as to how these set of activators/compounds might interfere with PP2A. The attempt was thus made to decipher the same via *in silico* docking analysis.

3.3 PP2A Pocket– activator Interactions

Docking analysis was carried out using known PP2A activators. The activators were selected based on the structural features comprising of different chemical classes which include Phenols, Anions, and Cations respectively. Phenolic class of activators contains Epigallocatechingallate, Dihydroxyphenylethano, Betatocopherol, Tetralone, Quinolone, and Methyl-3, 5-diiodo-4-(4'-methoxyphenoxy) benzoate, while the anionic class of activators were Xylulose-5-phosphate and Sodium selenate, respectively. Memantine was the only cationic class of activator that was selected.

The docking results revealed that the computationally predicted lowest energy ligand-complexes of PP2A are stabilized by intermolecular hydrogen bonds, hydrophobic and electrostatic interactions. All the activators were docked across Pocket 2 and Pocket 3

respectively, and showed interactions with key residues of PP2A, that are depicted in the **Table 6** and **Table 7** respectively.

It is clear that among all the 8 activators docked across pocket 2 comprising of 28 amino acid residues, Xylulose-5-phosphate, EpiGallocatechinGallate and DihydroxyPhenylethano, exhibit very strong interactions with 9 to 12 hydrogen bonds within 5.5Å, with good binding energies. Most of these activators have shown interactions with amino acid residues like E19, C20, E95, R294, R295, G296, E297,P298, H299, and V300 respectively, which are very much part of the pharmacophore. Sodium selenate and Quinolone showed strong interactions with 6 to 8 hydrogen bonds; while, Memantine, Beta Tocopherol and Tetralone exhibited moderate interactions with 3 to 5 hydrogen bonds. Thus the docking results suggest that Xylulose-5-phosphate, EpiGallocatechinGallate, DihydroxyPhenylethano, Memantine and Beta Tocopherol could be exploited as potential activators of PP2A.

Similarly, the Pocket 3 docking outcomes with these 8 selected activators illustrates interesting facts. Pocket 3 covers about 17 interacting amino acid residues, which display moderate to very strong interactions with these activators. The pharmacophoric residues of this pocket are illustrated in **Table 8**. Tetralone, which exhibited weak interaction with pocket 2 residues, displays very strong interaction with the pocket 3 residues. In spite of their higher binding affinities, Xylulose-5-Phosphate, Epigallocatechin Gallate and Dihydroxy Phenylethano showed moderate interactions in this case. However, Memantine and Sodium Selenate exhibit strong contacts here. Sodium Selenate, interestingly displays strong interaction in both the pockets, which could be explored as a potential dual pocket binder. Similarly, Beta Tocopherol showed strong interactions in pocket 3. Quinolone shows weak interactions in pocket 3, but appear to have strong bonding for pocket 2. Thus, with these evidences, Tetralone, Memantine,

Beta Tocopherol and Sodium Selenate could also be explored as potential activators of PP2A. Sodium Selenate appears to be the only common molecule exhibiting potential binding across both the pockets. The consolidated comparison between the strength of the interactions at pocket 2 and 3 are highlighted in the **Table 9**.

3.4 Side Chain Conformations and Flexibility

Our goal was to further analyze the conformational flexibility of the side chains atoms, across Phosphate binding site residues, as a function of the binding of ligand, inhibitor and activator molecules. The study involved determining the movements of the C alpha, side chain and all atoms of the PP2A, through the overlay assessment of the Toxin/activator bound complex structures. Analysis was carried out using molecular overlay function in DS 3.5. Docked complexes were assessed by measuring the inter-atomic distances from the Mn2+ metal ions, with the 9 active site amino acid residues. Details of this metal-amino acid interaction distances for the active site residues are presented in **Table 10**. Surprisingly, when the ligand and activator bound receptors were superimposed along with the native form (no ligand or inhibitor bound), the side chain amino acids of activator/ inhibitor bound forms showed interesting conformational changes. The amino acid side chains of ASP57, HIS59, ASP85, ASN117, HIS167, and HIS241 moved significantly at the metal and phosphate binding site, displaying significant variations in the bond distances. While, specific side chains of HIS 59, ARG 89, ARG 214, and HIS 241 experienced large movements compared to the native form, ASP85, ASP-97, and ASN-117 showed less rotations (refer **Figure 7 (A)(B)**). The amino acid residues of the inhibitor bound side chains tend to move inside the pocket, indicating that the ligand binding induces a strain in the side-chain conformations of active site residues of PP2A. However, in the case of activator bound form, the residues extend towards the outer side and generate more accurate side-chain

positions for triggering dephosphorylation activity. Thus, this position of activator bound form appears to coordinate in proper substrate binding and enable mediation of the dephosphorylation of Tau.

Similarly, our work emphasized to understand the overall conformational changes and the similarity of catalytic C subunit. Towards this, the RMSD calculations for C Alpha, Side-chain and all atoms of the 9 active site residues were carried out by choosing the native, toxin and inhibitor bound models. Details of these RMSD values are given in the **Table 11**. The RMSD of C alpha ranges from 0.39 Å to 0.65 Å; Side-chain RMSD ranges from 0.54 Å to 1.58 Å; and all atoms RMSD range from 0.75 Å to 1.38 Å, respectively.

Likewise, in order to appreciate the changes in the side chain orientation due to the toxin /activator binding at the catalytic C subunit, as case study 2 toxins and 2 inhibitors were considered for RMSD calculations.

The comparative results are illustrated in the **Table 12**. The data reveals that, the RMSD of C alpha ranges from 0.33 Å. to 0.79 Å; Side-chain values ranges from 0.35 Å to 1.92 Å and the same for all atoms ranges from 0.57 Å to 1.55 Å. These values, when compared to native form of PP2A specify that, the higher values of RMSD in the inhibitor bound form signifies that the peptide backbone and amino acid side-chains undergo drastic conformational changes upon ligand binding. Likewise, The RMSD value for activator bound forms indicate that, it is of 0.79 Å for C alpha; 1.77 Å for Side-chain atoms and 1.41 Å. for all atoms respectively.

It is evident that, from the comparative RMSD values for the native- activator form is less than the native – inhibitor form, indicating that the activator bound complex is closer to native conformation. The details of the binding energies and residues interacting at the catalytic c subunit are depicted in **Table 13**. This also highlights that, the activator D-Xylulose-5-Phosphate

and Epigallocatechin Gallate exhibit more preferential binding energy in comparison to inhibitor Okadaic acid and Fostriecin, interacting amino acids and their distance of interactions. In conclusion, these RMSD comparison efforts, suggest the changes in structure of catalytic C subunit orientation with the inhibitor/activator bound leading to the understanding of the PP2A regulation.

4. CONCLUSIONS

In this study we have considered four Tau Protein phosphatases involved AD. Extensive sequence and structural analysis were carried out to understand the conformational details of these phosphatases, as a result of inhibitor and activator binding, to their defined pockets. A molecular level appreciation of the nature of phosphate binding, inhibitor interactions and activators association to the pockets of PP2A has been provided. A set of 8 activators that pass the BBB were specifically docked to PP2A in order to decipher their superior selectivity and binding affinities. Among these 8 activator molecules, Xylulose-5-Phosphate, DihydroxyPhenylethano, Epigallocatechin Gallate, Memantine, Sodium Selenate, Tetralone and Quinolone appear to exhibit strong interactions with the pockets of PP2A, and show promise for exploration as potential therapeutic agents for AD.

5. CONFLICT OF INTEREST

The authors declare that there is no conflict of interests regarding the publication of this paper and the research was conducted in the absence of any commercial or financial relationships that could be construed as a potential conflict of interest.

6. AUTHOR CONTRIBUTIONS

 Jk jointly conceived the study with H.G.N; designed and implemented the protocol. Jk and MT conducted all bioinformatics analyses, collected and performed various *in silico* data and

analyzed; JK wrote the main paper, H.G.N. gave technical support and conceptual advice and supervised its analysis, P.N and H.G.N edited the manuscript; All authors discussed the results and implications and commented on the manuscript at all stages.

7. FUNDING

8. ACKNOWLEDGMENTS

9. REFERENCE

1. Kowalska A. Genetic basis of neurodegeneration in familial Alzheimer's disease. *Pol. J. Pharmacol.* 2004; 56: 171–178.

2. Lee G, Leugers CJ. Tau and Tauopathies. *Prog. Mol. Biol. Transl. Sci.* 2012; 107: 263–293. doi: 10.1016/B978-0-12-385883-2.00004-7

3. Klafki HW, Staufenbiel M, Kornhuber J, Wiltfang J. Therapeutic approaches to Alzheimer's disease. *Brain.* 2006; 129: 2840–55. doi: 10.1093/brain/awl280.

4. Chung S H. Aberrant phosphorylation in the pathogenesis of Alzheimer's disease. *BMB Rep* 2009; 42: 467–474.

5. Martin L, Latypova X, Wilson C. M, Magnaudeix A, Perrin M, Yardin C, Terro F, et al. Tau protein kinases : Involvement in Alzheimer's disease. *Ageing. Res. Rev.* 2013; 12:289–309. doi: 10.1016/j.arr.2012.06.003

6. Sontag JM, Sontag E. Protein phosphatase 2A dysfunction in Alzheimer's disease. *Front. Mol. Neurosci.* 2014; 7: (16):1-11. doi: 10.3389/fnmol.2014.00016.

7. Wang JZ, Xia YY, Grundke-Iqbal I, Iqbal K. Abnormal hyperphosphorylation of tau: Sites, regulation, and molecular mechanism of neurofibrillary degeneration. *Adv. Alzheimer's. Dis* 2012; 3: 123–139. doi: 10.3233/JAD-2012-129031

8. Kopke E, Tung Y, Shaikh S, Alonso A C, Iqbal K, Grundke-iqbals I, et al. Microtubule-associated Protein Tau Abnormal phosphorylation of a non-paired helical filament pool in Alzheimer disease. *J Biol. Chem* 1993; 18: 24374–24384.

9. Liu F. Grundke-Iqbal I, Iqbal K, Gong C X. Contributions of protein phosphatases PP1, PP2A, PP2B and PP5 to the regulation of tau phosphorylation. *Eur. J. Neurosci* 2005; 22: 1942–1950. doi: 10.1111/j.1460-9568.2005.04391.x

10. Shi Y. Serine/Threonine Phosphatases: Mechanism through Structure. *Cell*. 2009; 139: 468–484. doi: 10.1016/j.cell.2009.10.006.

11. Cho US, Xu W. Crystal structure of a protein phosphatase 2A heterotrimeric holoenzyme. *Nature*. 2007; 445: 53–57. doi: 10.1038/nature05351.

12. Xiong Y, Jing X , Zhou X W, Wang X L, Yang Y, Sun X Y, Qiu M, Cao F Y, Lu Y M, Liu R, Wang JZ, et al Zinc induces protein phosphatase 2A inactivation and tau hyperphosphorylation through Src dependent PP2A (tyrosine 307) phosphorylation. *Neurobiol. Aging*. 2013; 34: 745–56. doi: 10.1016/j.neurobiolaging.2012.07.003.

13. Liu R, Zhou X W, Tanila H, Bjorkdahl C, Wang J Z, Guan Z Z, Cao Y, Gustafsson J, Winblad B, Pei JJ, et al. Phosphorylated PP2A (tyrosine 307) is associated with Alzheimer neurofibrillary pathology. *J. Cell. Mol. Med.* 2008; 12: 241–57. doi: 10.1111/j.1582-4934.2008.00249.x

14. Himmelstein D S, Ward SM, Lancia J K, Patterson K R, Binder L I. Tau as a therapeutic target in neurodegenerative disease. *Pharmacol. Ther.* 2012; 136: 8-22. doi: 10.1016/j.pharmthera.2012.07.001

15. Voronkov M, Braithwaite S P, Stock JB. Phosphoprotein phosphatase 2A: a novel druggable target for Alzheimer's disease. *Futur. Med. Chem.* 2011; 3: 821–833. doi: 10.4155/fmc.11.47.

16. Xu Y, Chen Y, Zhang P, Jeffrey P D, Shi Y. Structure of a protein phosphatase 2A holoenzyme: insights into B55-mediated Tau dephosphorylation. *Mol. Cell.* 2008; 31: 873–85. doi: 10.1016/j.molcel.2008.08.006.

17. UniProt Consortium The Universal Protein Resource (UniProt). *Nucleic. Acids. Res.* 2010. 38 (Database issue),142–D148, doi: 10.1093/nar/gkp846

18. Berman H M, Westbrook J, Feng Z, Gilliland G, Bhat T N, Weissig H, Shindyalov IN, Bourne PE, et al The Protein Data Bank. *Nucleic. Acids. Res.* 2000; 1: 235-242.

19. Corpet F. Multiple sequence alignment with hierarchical clustering. *Nucl. Acids. Res.* 1988; 16: 10881-10890.

20. Robert X, Gouet P. Deciphering key features in protein structures with the new ENDscript server. *Nucleic. Acids. Res.* 2014; 42 Web Server issue, pp. W320–324. doi: 10.1093/nar/gku316.

21. Discovery studio (DS) (Discovery Studio 3.5, Accelrys Inc., San Diego, California, (http://www.accelrys.com/). USA).

22. Bingding Huang. MetaPocket: a meta approach to improve protein ligand binding site prediction. *Omics.* 2009; *13*: 325-330. doi: 10.1089/omi.2009.0045.

23. Kim S, Thiessen PA, Bolton E E, Chen J, Fu G, Gindulyte A, Han L, He J, He S, Shoemaker BA, Wang J, Yu B, Zhang J, Bryant S H, et al. PubChem Substance and Compound databases. *Nucleic. Acids. Res*. 2015, 2016; 4: 1202-1213. doi: 10.1093/nar/gkv951.

24. Gastreich et al (FlexX. http://www.biosolveit.de/FlexX/). 2006; St. Augustin, Germany.

25. Momany F A, Rone R J Validation of the general purpose QUANTA 3.2/CHARMm force field. *Comp. Chem.*1992; 13: 888-900.

26. Krammer A, Kirchhoff P D, Jiang X, Venkatachalam C M, Waldman M. LigScore: a novel scoring function for predicting binding affinities. *J. Mol. Graph.* Model. 2005; 23: 395-407. doi: 10.1016/j.jmgm.2004.11.007.

27. Honkanen R E, Codispoti B A, Tse K, Boynton A L, Honkanan R E. Characterization of natural toxins with inhibitory activity against serine/threonine protein phosphatases. *Toxicon,* 1994; 32: 339-350.

28. Xu Y, Chen Y, Zhang P, Jeffrey P D, Shi Y. Structure of a protein phosphatase 2A holoenzyme: insights into B55-mediated Tau dephosphorylation. *Mol. Cell*. 2008; 26: 873-885. doi: 10.1016/j.molcel.2008.08.006.

29. Ruediger R, Roeckel D, Fait J, Bergqvist A, Magnusson G, Walter G, et al Identification of Binding Sites on the Regulatory A Subunit of Protein Phosphatase 2A for the Catalytic C Subunit and for Tumor Antigens of Simian Virus 40 and Polyomavirus. *Mol. Cell. Biol.* 1992; 12: 4872–4882.

30. Sontag E, Luangpirom A, Hladik C, Mudrak I, Ogris E, Speciale S, White C. L, et al. Altered expression levels of the protein phosphatase 2A ABalphaC enzyme are associated with Alzheimer disease pathology. *J. Neuropathol. Exp. Neurol.* 2004; 63: 287–301.

31. Sontag E, Nunbhakdi-Craig V, Lee G, Bloom G S, Mumby M C. Regulation of the phosphorylation state and microtubule-binding activity of Tau by protein phosphatase 2A. *Neuron.* 1996; 17: 1201–1207.

32. Andrew M Slupe, Ronald A, Merrill, Stefan Strack. Determinants for Substrate Specificity of Protein Phosphatase 2A. *Enzyme. Research.* 2011; 2011: 398751.

33. Janssens V, Goris J. Protein phosphatase 2A, a highly regulated family of serine/threonine phosphatases implicated in cell growth and signaling. *Biochem. J.* 2001; 1: 417-439.

34. Groves MR, Hanlon N, Turowski P, Hemmings BA, Barford D. The structure of the protein phosphatase 2A PR65/A subunit reveals the conformation of its 15 tandemly repeated HEAT motifs. *Cell. 1996;* 8: 99-110.

35. Sontag J M, Sontag E. Protein phosphatase 2A dysfunction in Alzheimer's disease. *Front. Mol. Neurosci.* 2014; 11: 16. doi: 10.3389/fnmol.2014.00016.

36. Loring J F, Wen X, Lee J M, Seilhamer J, Somogyi R. A gene expression profile of Alzheimer's disease. *DNA. Cell. Biol.* 2001; 20: 683-695. doi: 10.1089/10445490152717541.

TABLES

Sl. No.	Short name of tau phosphatases/Gene name	Recommendedname/ Synonym	Uniprot ID	Protein Stoichiometry and No of chains present in proteins	PDB ID/catalytic chains	Number of Amino acids across catalytic chains
1.	PP1/PPP1CA	Serine/threonine-protein phosphatase PP1-alpha catalytic subunit	P62136 - PP1A_HUMAN	Monomer-A A(299)	3E7A/ A	299
2.	PP2A/PPP2CA	Serine/threonine-protein phosphatase 2A catalytic subunit alpha isoform	P67775- PP2AA_HUMAN	Hetero 3-mer – ABC A (582),B(447),C (309)	3DW8 /C	309
3.	PP2B/PPP3CA	Serine/threonine-protein phosphatase 2B catalytic subunit alpha isoform	Q08209- PP2BA_HUMAN	Hetero 2-mer – AB A(521),B(169)	1AUI/A	521
4.	PP5/PPP5C	Serine/threonine-protein phosphatase 5	P53041- PPP5_HUMAN	Monomer-A A (477)	1WAO/A	477

TABLE 1| List of human tau protein phosphatases implicated in AD, showing catalytic subunit, gene name, UniProtID, PDB ID and number of residues across catalytic subunit.

.	PP1 Catalytic subunit (3E7A)	PP2A Catalytic subunit (3DW8)	PP2B Catalytic subunit (1AUI)	PP5 Catalytic subunit (1WAO)
PP1 Catalytic subunit (PDB ID :3E7A)		-	-	-
PP2A Catalytic subunit (PDB ID :3DW8)	# I=50% / @ S=77% ∗ RMSD=0.93 C alpha Atoms=273	-	-	-
PP2B Catalytic subunit (PDB ID :1AUI)	I= 39% ,/ S= 71% RMSD=0.97 C alpha Atoms=264	I= 42 % / S= 67% RMSD=1.05 C alpha Atoms=270	-	-
PP5 Catalytic subunit (PDB ID :1WAO)	I= 40% / S= 69% RMSD=0.97 C alpha Atoms=265	I=41 % /S=71 % RMSD=1.06 C alpha Atoms=266	I= 37% / S= 67% RMSD=0.96 C alpha Atoms=270	-

TABLE 2| Showing the Percentage Identity, similarity, and RMSD values (for the overlapping number of atoms). #I represents Identity, @S denotes Similarity, and ∗denotes RMSD (along with total number of atoms involved) with catalytic subunits of Phosphatases.

Subunits	UniProt Entry/ Protein name	Gene names	Alternative names	Chromosome location
Catalytic C' subunit- alpha isoform	**P67775- P2AA_HUMAN** / Serine/threonine-protein phosphatase 2A,36kDa catalytic subunit alpha isoform	PPP2CA	Cα, PP2ACα, PP2a	5q31.1
Scaffold A' subunit- alpha isoform	**P30153- 2AAA_HUMAN**/ Serine/threonine-protein phosphatase 2A, 65 kDa regulatory subunit A alpha isoform	PPP2R1A	Aα subunit, PR65α	19q13.33
Regulatory B' subunit- alpha isoform	**P63151- 2ABA_HUMAN**/ Serine/threonine-protein phosphatase 2A,55kDa regulatory subunit B alpha isoform	PPP2R2A	Bα, B55α,R2α, PR55α, PP2A1	8p21.1

TABLE 3| Details of subunits, UniProt entry, gene name, Alternative names and Chromosome Location of Human protein phosphatase 2A (PP2A/Bα).

POCKET-2 AMINO ACID RESIDUES	POCKET-3 AMINO ACID RESIDUES
D11,Q12,E15,Q16,N18,E19,C20,S24,Q61,F62, H63,D64,L65,M66,E67,L68,F69,R70,G73,K74,S75,P76,G90,Y91,Y92,E95,L99,L103,R106,Y107,Y130,D131,E132,L134,R135,K136,Y137,G138,N139,N264,Y265,C269,A292,P293,R294,R295,G296,E297,P298,H299,V300,T301,T304,P305,D306, Y307,F308. - 58	S120,R121,Q122,I123,Q125,V126,Y127,W143,E188,V189,P190,H191,E192,C196,W200,G215,A216.-17

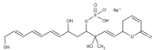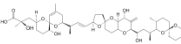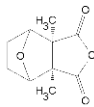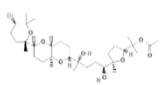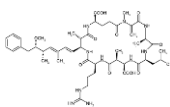**TABLE 4|** showing amino acid residues across predicted three pockets.

SL NO	INHIBITORS OF PP2A	STRUCTURAL SCAFFOLD AND MOLECULAR DETAILS	SELECTIVITY	ISOLATION ORIGIN	AMINO ACIDS RESIDUES INTERACTING AND HYDROGEN BOND DISTANCES	INTERACTION ENERGY	CHEMICAL STRUCTURES OF LIGANDS
1.	FOSTRIECIN	Polyketide PubChem CID: 6913994 MF:C19H27O9P	Is a selective PP2A inhibitors	*Streptomyces pulveraceus*	ARG-89-2.587 GLY193-3.190 GLN122-3.254 HIS118-3.549 ARG214-2.019 PRO213-3.162 SER212-3.225 GLY217-3.301 LEU-243-3.816 CYS-269-3.568	-14.3191	
2.	OKADAIC ACID	Polyketide, MF-$C_{44}H_{68}O_{13}$ ChemSpider :ID393845	Is a selective PP2A inhibitors	*Dinoflagellates*	ARG-89-3.750 GLY193-3.162 ARG214-3.189 GLY217-3.055 LEU-243-3.162 MET-245-3.547 TYR-248-3.896 GLn288-2.854	-11.3375	
3.	CANTHARIDIN	Terpenoid PubChem CID: 5944 MF-$C_{10}H_{12}O_4$	Is a selective PP2A inhibitors	Blister beetles	ARG89-3.669 TYR127-3.914	-10.1827	
4.	THYRSIFERYL-23-ACETATE	Terpenoid PubChem CID:125904 MF:C32H55BrO8	Is a selective PP2A inhibitors	Red algae, *L. Obtusa*	TYR127-2.811 HIS 191-3.062 GLY193-2.201 SER212-2.342 ARG-214-3.503 GLY217-2.443 GLN-242-2.856	-7.4855	
5.	MICROCYSTINS- LR	Cyclic peptide MF- $C_{49}H_{74}N_{10}O_{12}$ PubChem CID:445434	Is a potent inhibitors of PP1 and PP2A, But poor PP2B and PP2C inhibitors.	Blue green algae	TYR127-2.811 HIS191-3.787 TYR265-3.946 ARG268-2.340	-0.145	

TABLE 5| showing molecular details of selective natural toxin inhibitors of PP2A and their docking scores with PP2A.

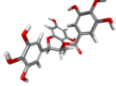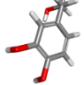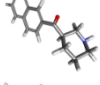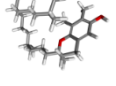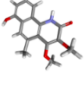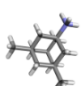| Sl NO	CLASS AND NAME OF ACTIVATOR	PUBCHEM CID AND MOLECULAR FORMULA	MOLECULAR WEIGHT (g/mol)	xlogP	CHEMICAL STRUCTURE
1.	Anionic class : D-XYLULOSE-5-PHOSPHATE	439190 C5H11O8P	230.109802 g/mol	-3.74	
2.	Phenolic class: (-) -EPIGALLOCATECHIN GALLATE	65064 C22H18O11	458.37172 g/mol	2.25	
3.	Phenolic class : DIHYDROXYPHENYLETHANO [DROXYTYROSOL]	82755 C8H10O3	154.1632 g/mol	0.52	
4.	Anionic class: SODIUM SELENATE	25960 Na2O4Se	172.937739 g/mol	---	
5.	Phenolic class : TETRALONE	56744489 C16H17NO	239.31228 g/mol	---	
6.	Phenolic class : β-TOCOPHEROL	6857447 C28H48O2	416.67952 g/mol	9.67	
7.	Phenolic class : QUINOLONE	10356576 C16H15NO4	285.2946 g/mol	---	
8.	Cationic class : MEMANTINE- (MemantineCation)	3833001 C12H22N	180.30978	2.77	

TABLE 6| Showing the class of activators and their details used for docking studies

POCKET2 - Interacting Amino acid residues- 28	XYLULOSE-5-PHOSPHATE	EPI GALLOCATECHIN GALLATE	DIHYDROXY PHENYLETHANO	SODIUM SELENATE	TETRALONE	BETA TOCOPHEROL	QUINOLONE	MEMANTINE	# of common interacting residues across all ligands
D11	6.011	-	-	-	-	-	-	-	0+1
Q12	4.403	-	-	-	-	-	-	-	1+0
E15	3.346	-	-	-	-	-	-	-	1+0
Q16	3.109	5.909	-	-	-	-	-	-	1+1
N18	2.475	2.549	-	-	-	-	-	-	3+0
E19	4.400	3.280	-	-	5.813	-	-	6.02	3+2
C20	5.631	2.445	-	-	2.567	-	-	2.655	4+1
Q61	-	-	-	3.517	-	-	-	-	1+0
H63	-	3.695	5.682	-	-	-	-	-	2+1
D64	-	-	-	3.582	-	-	-	-	1+0
E67	-	6.00	-	-	-	-	-	-	0+1
R70	-	6.01	-	-	-	-	-	-	0+1
Y92	-	-	5.651	-	-	-	4.551	-	1+1
E95	2.822	-	-	-	2.808	-	-	2.592	3+0
L99	3.576	-	-	-	-	-	-	-	1+0
K136	-	-	-	-	-	-	-	4.121	1+0
N264	-	-	-	3.04	-	-	-	-	1+0
Y265	-	-	-	4.117	-	-	-	-	1+0
A292	-	4.995	-	4.795	-	-	-	-	2+0
P293	-	3.222	5.605	-	-	-	-	-	1+1
R294	-	2.886	4.699	2.615	-	-	5.425	-	4+0
R295	-	2.688	2.614	-	-	5.547	3.050	-	3+1
G296	-	4.875	2.501	-	-	5.519	4.633	-	3+1
E297	-	-	4.659	-	-	5.377	5.557	-	2+1
P298	-	-	2.579	-	-	3.154	5.209	-	3+0
H299	-	-	3.131	-	-	5.437	4.685	-	3+0
V300	-	-	3.321	-	-	-	4.627	-	2+0
T301	-	-	5.633	-	-	-	-	-	0+1
# H-bonds around 6A^0 (5.5+.-0.5)	7+2	9+3	7+4	6+0	2+1	3+2	7+1	3+1	-
Binding energy	-27.424	-24.443	-16.267	-12.225	-12.767	-11.75	-8.899	-6.639	
Probable Strength of interaction	Very Strong	Very Strong	Very Strong	Strong	Moderate	Moderate	Strong	Moderate	-

TABLE 7| POCKET 2- Interacting Amino acid residues of PP2A with activators - around 6 Å (5.5+0.5)

POCKET 3- Interacting Amino acid residues-17	EPIGALLOCATECHIN GALLATE	TETRALONE	XYLULOSE-5-PHOSPHATE	DIHYDROXY PHENYLETHANO	MEMANTINE	QUINOLONE	BETA TOCOPHEROL	SODIUM SELENATE	# of common interacting residues across all ligands
S120	2.537	3.627	2.633	4.519	4.904	4.507	2.738	2.732	8+0
R121	5.589	5.155	3.309	-	4.638	-	3.292	2.911	4+2
Q122	2.773	4.282	5.962	-	3.017	-	4.975	4.651	5+1
I123	4.496	5.082	4.903	-	5.093	-	5.100	5.041	6+2
Q125	-	-	3.584	-	-	-	3.586	3.397	3+0
V126	-	-	-	-	-	-	-	5.089	1+0
Y127	-	-	-	-	-	-	-	-	2+0
W143	-	-	-	-	-	-	3.054	3.021	2+0
E188	-	2.757	-	-	2.810	-	-	-	2+0
V189	-	2.806	-	-	4.119	-	-	-	2+0
P190	-	4.951	-	-	-	-	-	-	4+0
H191	-	4.93	-	3.538	-	-	-	-	2+0
E192	-	-	-	5.724	-	-	-	-	0+1
C196	-	-	-	5.470	-	2.553	-	-	1+1
W200	-	5.611	-	2.979	-	2.365	-	-	2+1
G215	-	-	-	-	-	-	-	-	0+0
A216	-	-	-	-	-	-	-	-	0+0
# H-bonds around 6A^0 (5.5+.-0.5)	3+1	6+3	4+1	3+2	5+1	3+0	5+1	5+2	-
Binding energy	-21.614	-16.698	-15.711	-14.89	-12.368	-11.582	-10.206	-8.162	
Probable Strength of interaction	MODERATE	VERY STRONG	MODERATE	MODERATE	STRONG	MODERATE	STRONG	STRONG	

TABLE 8| POCKET3- Interacting Amino acid residues of PP2A with activators - around 6Å (5.5+0.5)

ACTIVATORS # H-bonds around 6A (5.5+0.5)	XYLULOSE-5-PHOSPHATE	-(-)EPI GALLOCATECHIN GALLATE	DIHYDROXYPHENYL ETHANO	SODIUM SELENATE	TETRALONE	BETATOCOPHEROL	MEMANTINE	QUINOLONE
POCKET 2	7+2	9+3	7+4	6+0	2+1	3+2	3+1	7+1
STRENGTH OF INTERACTION	VERY STRONG	VERY STRONG	VERY STRONG	STRONG	WEAK	MODERATE	MODERATE	STRONG
Binding energy	-27.424	-24.443	-16.267	-12.225	-12.767	-11.75	-6.639	-8.899
POCKET 3	4+1	3+1	3+2	5+2	6+3	5+1	5+1	3+0
Binding energy	-15.711	-21.614	-14.89	-8.162	-16.698	-10.206	-12.368	-11.582
STRENGTH OF INTERACTION	MODERATE	MODERATE	MODERATE	STRONG	VERY STRONG	MODERATE	STRONG	WEAK

TABLE 9| Comparative table for activators docking with PP2A indicating the strength of the interaction - AROUND 6 Å (5.5+0.5)

SL no	Residues interacting with Mn2+	Native form distances with Mn2+	Okadaic Acid Toxin Bound distances with Mn2+	Fostriecin Toxin Bound distances with Mn2+	Activator Xylulose Bound distances with Mn2+	Activator EGCGBound distances with Mn2+
1.	ASP57	2.133	2.042 / 2.698	2.042 / 2.698	2.265 / 3.988	2.278 / 4.018
2.	HIS59	2.330	2.607	2.607	2.800	2.834
3.	ASP85	1.966 / 2.399	2.195 / 2.589	2.495 / 2.589	2.384 / 3.401	2.434 / 3.427
4.	ASN117	2.053	2.541	2.541	3.205	3.224
5.	HIS167	2.128	1.840	1.840	2.013	2.064
6.	HIS241	2.213	3.451	3.451	4.114	4.169

TABLE 10| showing the distances of amino acid interacting with and $Mn2^+$ metal ion across active site

	NATIVE	OKADAIC ACID	FOSTRIECIN	D-XYLULOSE-5-PHOSPHATE	EPIGALLOCATECHIN GALLATE
NATIVE	-----	-----	-----	-----	-----
OKADAIC ACID	C Alpha -0.65-(9) Side-chain-1.28--(43) All Atoms -1.18-(75)	------	-----	-----	-----
FOSTRIECIN	C Alpha -0.65 --(9) Side-chain-1.58--(43) All Atoms -1.38-(75)	C Alpha -0.25 --(9) Side-chain-0.54--(50) All Atoms -0.75--(86)-	-----	-----	-----
D-XYLULOSE-5-PHOSPHATE	C Alpha -0.61--(9) Side-chain-1.07-(43) All Atoms -1.02-(75)	C Alpha -0.65 (9) Side-chain-1.28(43) All Atoms -1.18(75)	C Alpha -0.60--(9) Side-chain-1.18-(43) All Atoms -1.38(75)	------	-----
EPIGALLOCATECHIN GALLATE	C Alpha -0.61--(9) Side-chain-1.15-(43) All Atoms -1.12-(75)	C Alpha -0.42-(9) Side-chain-1.13-(50) All Atoms -0.91-(86)	C Alpha -0.39--(9) Side-chain-1.25--(50) All Atoms -1.12-(86)	C Alpha -0.61--(9) Side-chain-1.07-(43) All Atoms -1.02-(75)	-----

TABLE 11| RMSD Report of 9 active site residues.

	NATIVE	OKADAIC ACID	FOSTRIECIN	D-XYLULOSE-5-PHOSPHATE	EPIGALLOCATECHIN GALLATE
NATIVE	-----	-----	-----	-----	-----
OKADAIC ACID	**Calpha** **NBI- 284** **RMS-0.93** **Side chain** **NBI-1147** **RMS-1.92** **All atoms** **NBI-2283** **RMS-1.55**	-----	-----	-----	-----
FOSTRIECIN	**Calpha** **NBI- 284** **RMS-0.93** **Side chain** **NBI-1147** **RMS-1.92** **All atoms** **NBI-2283** **RMS-1.55**	**Calpha** **NBI- 284** **RMS-0.43** **Side chain** **NBI-1147** **RMS-0.55** **All atoms** **NBI-2283** **RMS-0.57**	-----	-----	-----
D-XYLULOSE-5-PHOSPHATE	**Calpha** **NBI- 284** **RMS-0.79** **Side chain** **NBI-1147** **RMS-1.77** **All atoms** **NBI-2283** **RMS-1.41**	**Calpha** **NBI- 306** **RMS-0.71** **Side chain** **NBI-1251** **RMS-1.40** **All atoms** **NBI-2283** **RMS-1.41**	**Calpha** **NBI- 306** **RMS-0.71** **Side chain** **NBI-1251** **RMS-1.40** **All atoms** **NBI-2471** **RMS-1.14**	-----	-----
EPIGALLOCATECHIN GALLATE	**Calpha** **NBI- 284** **RMS-0.79** **Side chain** **NBI-1147** **RMS-1.77** **All atoms** **NBI-2283** **RMS-1.41**	**Calpha** **NBI- 306** **RMS-0.71** **Side chain** **NBI-1251** **RMS-1.40** **All atoms** **NBI-2471** **RMS-1.14**	**Calpha** **NBI- 306** **RMS-0.71** **Side chain** **NBI-1251** **RMS-1.40** **All atoms** **NBI-2471** **RMS-1.14**	**Calpha** **NBI- 284** **RMS-0.33** **Side chain** **NBI-1147** **RMS-0.35** **All atoms** **NBI-2283** **RMS-0.88**	------

Table 12| Table showing the RMSD comparison of C alpha subunit docked with Toxin and activators.

SL no	Residues interacting with Mn2+	Binding free energy	Amino acid interacting
1.	FOSTRIECIN	-11.3191	G193-3.190, P213-3.162, S212-3.225, R214-2.019, G217-3.301, G217-2.507
2.	OKADAIC ACID	-5.3375	Q122-3.750, G193-3.162, R214-3.189, G217-3.055
3.	D-XYLULOSE-5-PHOSPHATE	-27.424	D11-6.011, Q12,-4.403, E15-3.346, Q16-3.109, N18-2.475, E19-4.400, C20-,5.631, E95-2.822, L99-3.576
4.	EPIGALLOCATECHIN GALLATE	-24.443	Q16-5.909, N18-2.549, E19-3.280, C20-2.445, H63-3.695, E67-6.00, R70-6.01, A292-4.995, P293-3.222, R294-2.886, R295-2.688, G296-4.875

Table 13| Showing the Comparison of binding energies and amino acid residue interacting (along with distances) with respective Toxins and Activators chosen for the study.
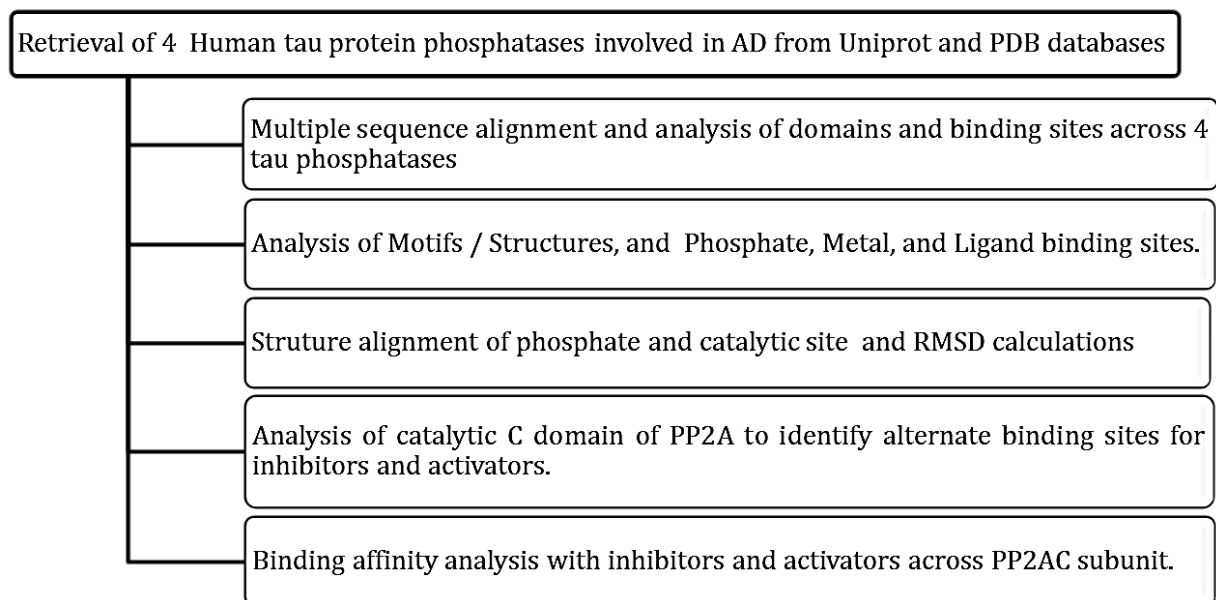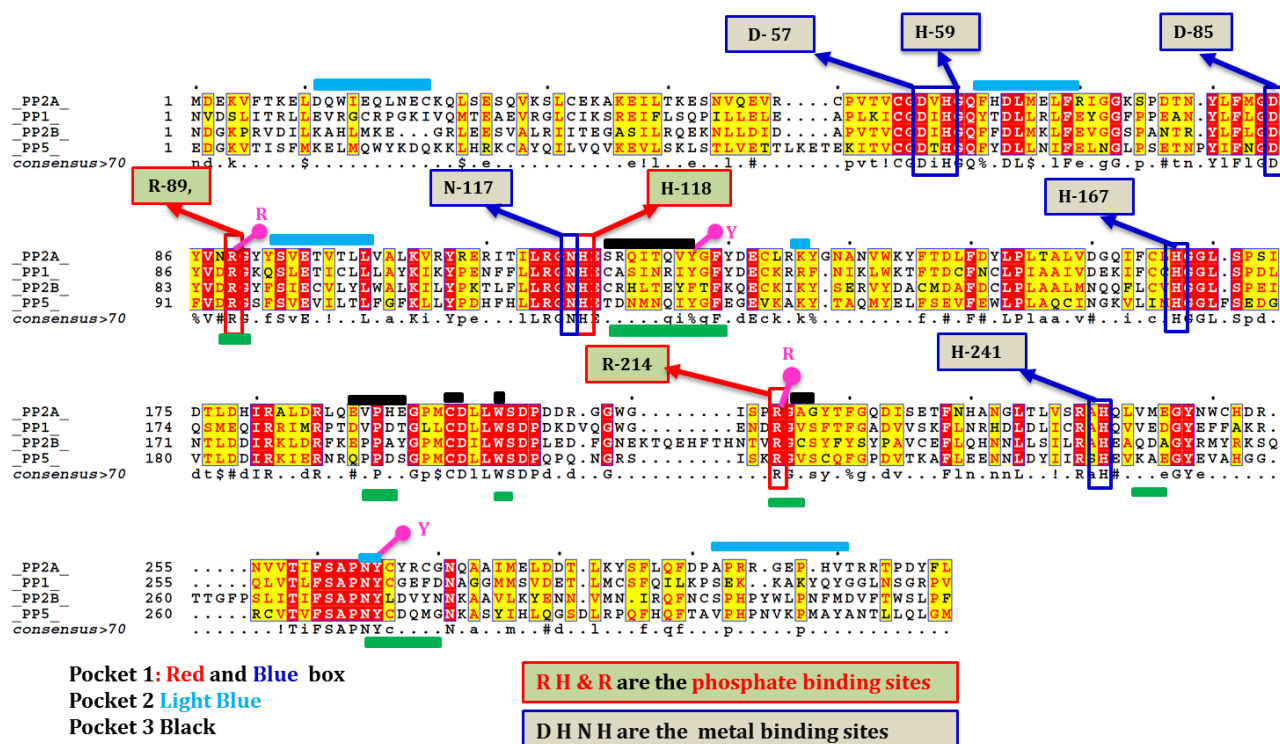
FIGURES

Retrieval of 4 Human tau protein phosphatases involved in AD from Uniprot and PDB databases

Multiple sequence alignment and analysis of domains and binding sites across 4 tau phosphatases

Analysis of Motifs / Structures, and Phosphate, Metal, and Ligand binding sites.

Struture alignment of phosphate and catalytic site and RMSD calculations

Analysis of catalytic C domain of PP2A to identify alternate binding sites for inhibitors and activators.

Binding affinity analysis with inhibitors and activators across PP2AC subunit.

FIGURE 1| Work Flow Chart

FIGURE 2| Multiple sequence alignment with hierarchical clustering analysis of catalytic C domains of tau Protein phosphatases PP2A, PP1, PP2B, and PP5. Strictly conserved residues among the four molecules are highlighted in red and highly conserved residues are indicated by yellow. Amino acids **RH&R** are conserved key Phosphate binding sites shown in red box and four-conserved **DHNH** amino acids are metal coordination substrate contacts shown in blue box across catalytic site, shared by PP2A, PP1, PP2B and PP5. Amino acid residues that form hydrogen bond and Van der Waals contact with toxins are highlighted in green color. Residues highlighted in pink color forms high affinity interaction with inhibitor. Pocket 2 and Pocket 3 comprising residues are presented as Light Blue and Black lines respectively.
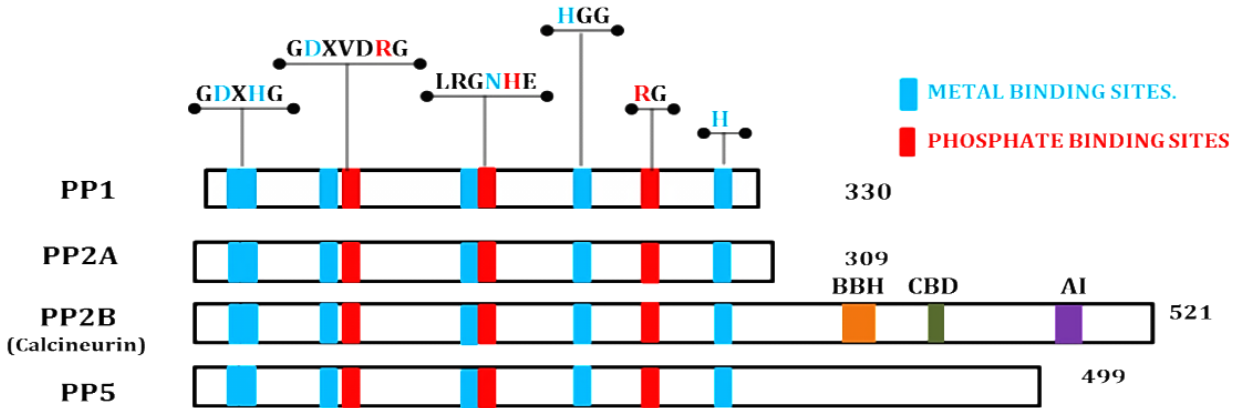
FIGURE 3| Diagram describes the catalytic core domain active site signature sequence motifs depiction of Human Tau phospho protein phosphatases (PPPs)
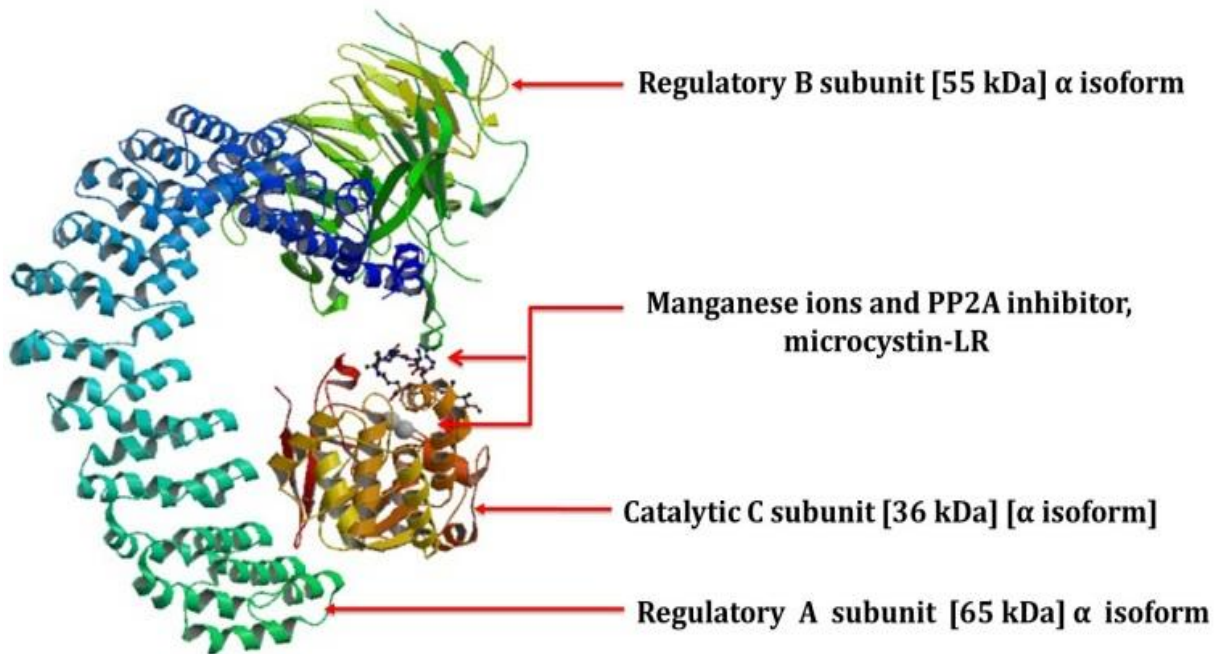.

FIGURE 4| The three subunit structure of heterotrimericholoenzyme Protein Phosphatase 2A (PP2A/Bα) (PDB ID: 3DW8).The Regulatory A subunit recruits the C catalytic subunit to form the core dimer, which acts as a support for the C and B subunits of the enzyme. Catalytic C subunit indicates the presence of manganese ions and is stabilized by a PP2A inhibitor, microcystin-LR.
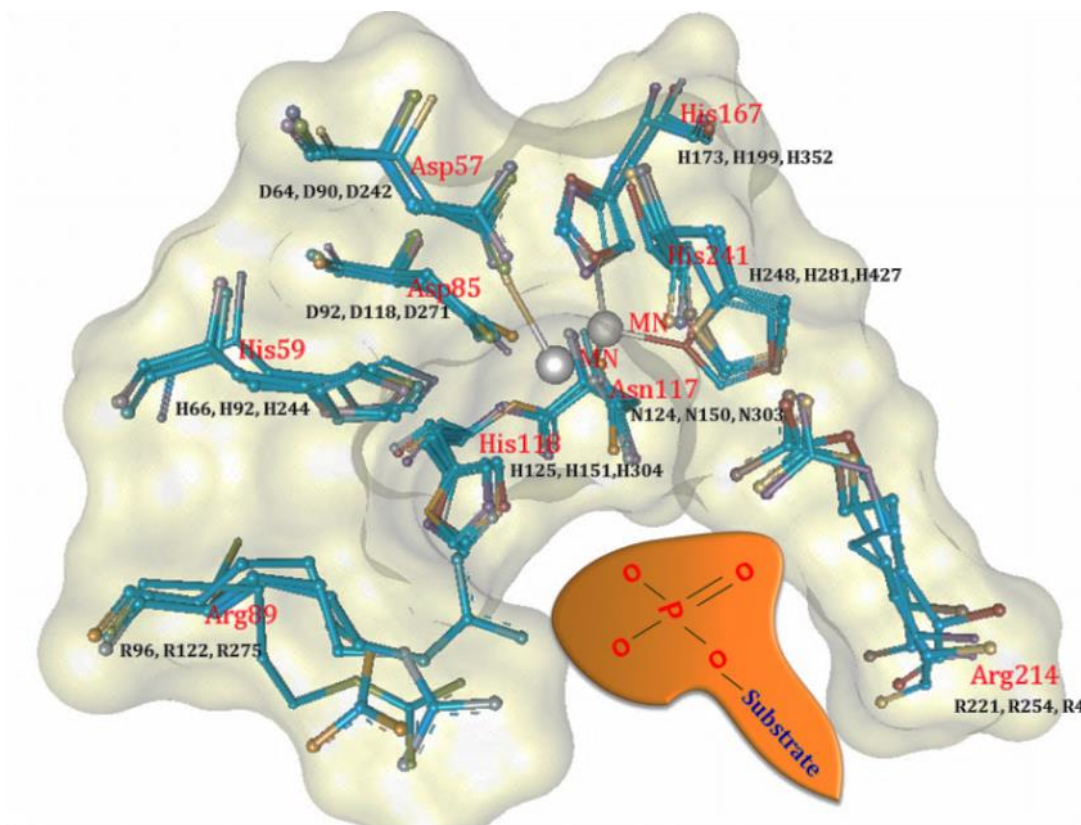
FIGURE 5| Superposition of catalytic C domain of 4 Human tau phosphatases PP1-(PDB ID: 3E7A), PP2A-(PDB ID:3DW8), PP2B-(PDB ID:1AUI) and PP5-(PDB ID: 1WAO) showing the 9 conserved active site amino acid residues in ball & stick representation along with the substrate binding site.
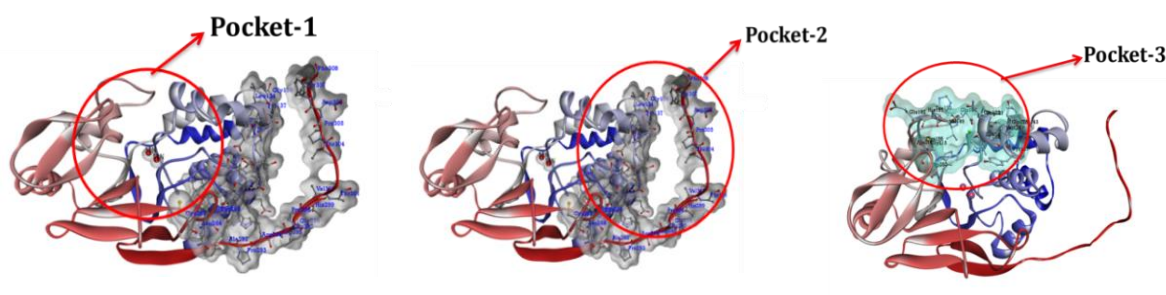

FIGURE 6| Toxin and phosphate binding site (Pocket 1) and 2 different pockets (pocket 2 and pocket3) identified across PP2A.
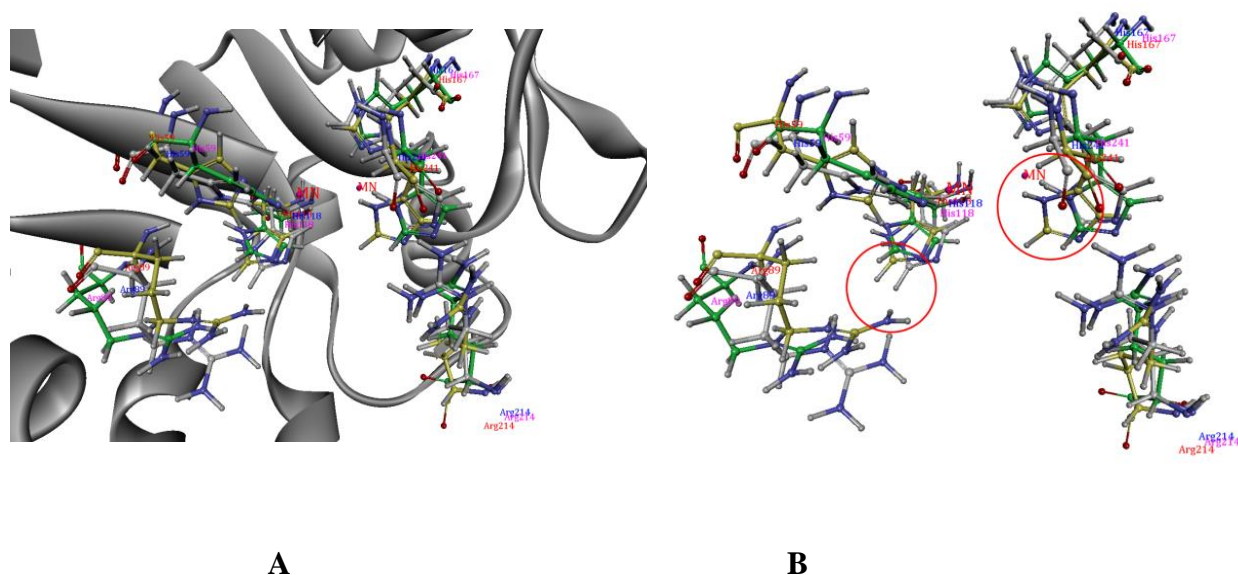
A   **B**

FIGURE 7| Overlay comparison of Mn2$^+$ distances of Okadaic acid with EGCG and Native form of PP2A, Exhibiting the changes in the side chain positioning and variation in the bond distances of amino acid is interacting with Mn2$^+$ metal ion across active site of PP2A. (Amino acid colored with Lime green carbon atom - native, with yellow-Okadaic acid bound and- white with EGCG Bound **(A)**. Showing the position of side chains of HIS 59, ARG 89 ARG 214, and HIS 241 of native with activator / inhibitor. The circles in the picture highlights probable steric collisions with the ligand bound conformation **(B)**.